DOI: https://doi.org/10.15407/pmach2020.04.038

UDC 539.3

ANALYSIS OF CRACK GROWTH IN THE WALL OF AN ELECTROLYSER COMPARTMENT

Pavlo P. Hontarovskyi
gontarpp@gmail.com
ORCID: 0000-0002-8503-0959

Natalia V. Smetankina
nsmetankina@ukr.net
ORCID: 0000-0001-9528-3741

Nataliia H. Garmash
garm.nataly@gmail.com
ORCID: 0000-0002-4890-8152

Iryna I. Melezhyk
melezhyk81@gmail.com
ORCID: 0000-0002-8968-5581

A. Pidhornyi Institute of Mechanical Engineering Problems of NASU,
2/10, Pozharskyi St.,
Kharkiv, 61046, Ukraine

Electrolysis units are widely used in different branches of industry. They are high-pressure tanks, each having a chamber and electrodes placed therein, which are arranged in assemblies, a cover as well as an inlet and outlet pipes. High requirements are imposed on their technical characteristics, confirming the urgency of the problem of improving calculation methods. To simulate the kinetics of the thermally stressed state in elements of power plants with complex rheological characteristics of the material and taking into account its damageability, a special technique and software complex have been developed on the basis of the finite element method, which allow solving a wide class of nonlinear nonstationary problems in a three-dimensional formulation with simultaneous consideration of all operating factors. The kinetics of the crack was studied using the method of calculating the survivability of structural elements, which is based on the principles of brittle fracture mechanics, while the plastic zone at the crack tip is assumed to be small compared to the crack size, and the crack kinetics is determined by the stress intensity factors at crack tips. The technique is based on calculating the kinetics of the crack to its critical dimensions, when an avalanche-like destruction of a structural element occurs, or a crack grows through the thickness of the element. The kinetics of a semi-elliptical crack emerging on the inner surface of the cell wall was studied under the action of static and cyclic loading. With the use of the developed technique, computational studies of the thermal stress state of the upper part of the electrolyser cell were carried out. The results obtained show that the cylindrical part of the cover is the most loaded. There have been carried out studies of the development of an internal surface semi-elliptical crack, which originated in this zone. It was found that with a small number of cycles per year, the crack will grow for a long time to a certain depth, then the rate of its growth from static loading will increase so quickly that the growth of the crack from cyclic loading can be neglected.

***Keywords**: electrolyser, hydrogenation, stress-strain state, medium, crack.*

Introduction

Electrolysis units and the hydrogen they produce are widely used in different branches of industry. Typically, electrolysers are manufactured as high-pressure tanks, each having an electrolysis compartment with electrodes installed therein. The electrodes are combined in assemblies with the active and passive electrodes being arranged alternately and mounted rigidly onto current leads. With such a scheme, the passive electrodes are connected to the casing, and the active ones, to the current conductor. The structure also includes a cover as well as inlet and outlet pipes [1].

The initiation of fatigue cracks and their growth due to hydrogen embrittlement of structural materials in contact with the hydrogen-containing medium is studied in papers [2–7].

The strict requirements to the technical characteristics of such structures attest to the relevance of the problem of refining their design methods. A valid evaluation of the performance capability of structures under thermal force loading is possible if one uses numerical simulation of the changes in their stress-strain state with simultaneous consideration of all acting factors.

Problem Statement

A special technique and a software package based on the finite element method (FEM) were developed to simulate the kinetics of the thermal stress state in power installation components with complex rheological properties of a material with account of its failure. A three-dimensional statement is used to solve a wide class of nonlinear unsteady problems with a rather low computational burden [8, 9].

When developing computational schemes, the system for specifying the source data is based on the topologically regular decomposition of a body into macro elements in the form of arbitrary hexahedrons the geometry

and external action on which can be specified in different coordinate systems (Cartesian, cylindrical, spherical, and toroidal) oriented arbitrarily with respect to the global Cartesian coordinate system. Based on the given information, the software complex automatically discretizes the hexahedrons into simplest finite elements.

The properties of the materials of the structure depend on temperature, and are specified as tables for its fixed values. For other temperature values, the properties are defined using linear or quadratic interpolation.

An arbitrary number of kinds of boundary conditions is specified. These boundary conditions are then distributed over the faces of macro elements. The boundary condition number is designated for each subdomain face. The boundary condition components can change with coordinates and time, and they are specified using special functions for fixed time instances. Boundary conditions of the second and third kind, as well as radiant heat transfer are specified for the heat conduction problem. Components of stresses or displacements in the global or local system of coordinates are specified for the mechanics problem. Volume heat sources and drains as well as different kinds of loads are also specified. The initial conditions are specified by constant values or obtained by solving the stationary problem for given boundary conditions.

Research Methodology

The initial boundary-value problem is solved using the time-step method. In so doing, explicit and implicit finite-difference schemes with automated step selection are used. Each step allows for an iteration process to find the parameters of linearized problems. To compute the thermophysical properties of the material, a temperature forecast is allowed, which helps save one iteration.

The axisymmetrical unsteady heat conductance problem is solved in the cylindrical system of coordinates by using the functional [8]

$$I = \frac{1}{2}\iint\limits_S \left[k_r\left(\frac{\partial T}{\partial r}\right)^2 + k_z\left(\frac{\partial T}{\partial z}\right)^2 + k_{rz}\cdot\frac{\partial T}{\partial r}\cdot\frac{\partial T}{\partial z} + 2QT - 2\rho c\cdot\frac{\partial T}{\partial t}\cdot T \right] rdS - \int\limits_{L_q} qTrdL + \int\limits_{L_\alpha} \alpha\cdot\left(\frac{T}{2} - T_\infty\right) TrdL,$$

where $k_r(T)$, $k_z(T)$, $k_{rz}(T)$ are thermal conductivity coefficients; $Q(r, z, t)$ is the intensity of internal heat sources; $\rho c(T)$ is the volumetric specific heat of the material; q is the intensity of heat flux across the boundary L_q; α, T_∞ is heat transfer coefficient and medium temperature on boundary L_α.

In this case, the implicit Crank-Nicolson scheme is used [8]

$$\frac{\partial T(t+\Delta t)}{\partial t} = (T(t+\Delta t) - T(t))\cdot\frac{2}{\Delta t} - \frac{\partial T(t)}{\partial t}.$$

The mechanics problem statement is based on the incremental variant of the Lagrange variational principle with modified tensors of Kirchhoff's stresses and Green's strains, for which the variation of the respective functional has the form [8]

$$\iiint\limits_V \left[(\sigma_{ij} + \Delta\sigma_{ij})\delta e_{ij} - (F_i + \Delta F_i)\delta\Delta u_i \right] dV - \iint\limits_S (P_i + \Delta P_i)\delta u_i dS = 0, \quad (1)$$

where σ_{ij} is Euler's stress tensor defined in the initial coordinate system at the beginning of the step, with the tensor being in equilibrium with applied mass forces F_i and surface forces P_i referred to unit volume V; ΔF_i, ΔP_i are increments of forces that cause body strain and the initiation of increments of displacements Δu_i, strains Δe_{ij} and stresses $\Delta\sigma_{ij}$.

Linearising equation (1) and physical law relationships

$$\Delta\sigma_{ij} = C_{ijkl}\Delta\varepsilon_{kl} + \sigma^0_{ij},$$

where $\Delta\varepsilon_{kl}$ is the tensor of increment of total strains, found from Cauchy relationships; C_{ijkl} is material elasticity tensor; σ^0_{ij} is stress at the beginning of the step. Then by applying the usual FEM procedure, we obtain a linear system of resolving equations for the finite element.

The tensor of increment of total strains $\Delta\varepsilon_{ij}$ is represented as a sum of elastic components $\Delta\varepsilon^e_{ij}$ and temperature components $\Delta\varepsilon^T_{ij}$

$$\Delta\varepsilon_{ij} = \Delta\varepsilon^e_{ij} + \Delta\varepsilon^T_{ij}.$$

The elastic strain increment is defined by Hooke's law

$$\Delta\varepsilon^e_{ij} = A_{ijkl}\Delta\varepsilon_{kl} + \Delta A_{ijkl}\varepsilon_{kl},$$

where A_{ijkl} is tensor of elastic material compliance at the temperature at the end of the step; ΔA_{ijkl} is the tensor of increment of elastic material compliance in a step due to a temperature change.

The increment of temperature strains is defined by the relationship

$$\Delta\varepsilon_{ij}^{T} = \alpha_i^{(2)} T^{(2)} - \alpha_i^{(1)} T^{(1)},\ \Delta\varepsilon_{ij}^{T} = 0,\ i \neq j,$$

where α_i are coefficients of linear temperature expansion of the material. Superscripts 1 and 2 designate the values at the beginning and end of the step.

The system of linear FEM equations is solved using the square-root method with account of the variable semistrip width. The coefficients of the system of equations are calculated using Gauss binodal quadratures.

Modified strain and stress tensors enable using conventional elasticity and creep theories because in this case the conditions of material incompressibility will be satisfied approximately. The algorithm is simplified considerably when solving problems for large displacements but small strains.

Depending on the geometrical complexity of the structure whose thermal stress state is to be simulated, plane, axisymmetrical and three-dimensional models can be used. In this study, the axisymmetrical computational scheme for the upper part (cover) of the electrolyser cell was used.

Results

The method developed was used in the computational analysis of the thermal stress state of the upper part (cover) of an electrolyser cell. The cylindrical part of the electrolyser cell is under an internal pressure of P=15 MPa and has a volume of 40 litres, with a wall thickness of h=7 mm. Fig. 1 is the computational scheme for the symmetrical part of the cover with finite-element discretization.

Figs. 2–4 are the profiles of stress intensities and of axial and circumferential stresses, respectively. They show that the cylindrical part of the cover is the most loaded one. The propagation of the internal surface of semi-elliptical crack that initiated in this zone will be analysed. Since the circumferential stresses σ_θ significantly exceed the axial ones σ_Z, the meridional crack is more dangerous than the annular one.

Fig. 5 is the cross-section of the structural element with a surface semi-elliptical crack with depth l and width c. The computational domain is a rectangle with width b and thickness h. The loading is specified by an arbitrary stress diagram along the crack depth l.

Crack kinetics was studied using the technique of computational estimate of the durability of structural components [8, 10]. The technique is based on principles of brittle fracture mechanics, with the zone of plasticity in the crack tip supposed to be small as compared to crack dimensions. The crack kinetics is governed by the stress intensity factors (SIF) in its tips.

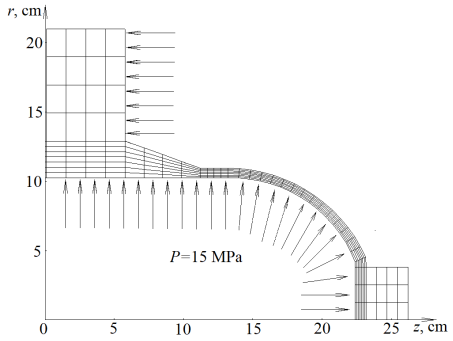

Fig. 1. Computational scheme for the symmetrical part of the cover with finite-element discretization

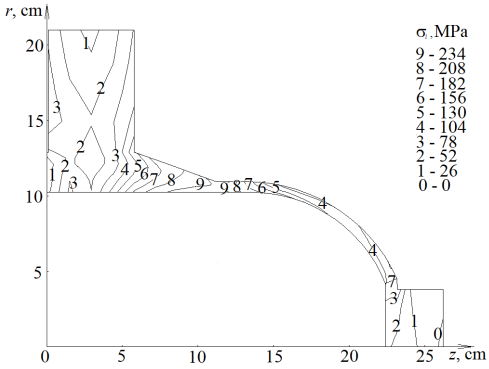

Fig. 2. Pattern of stress intensities σ_i

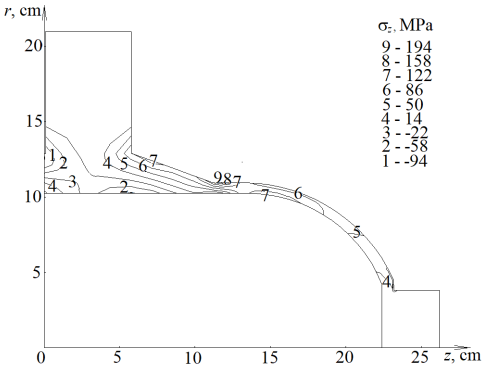

Fig. 3. Pattern of axial stresses σ_Z

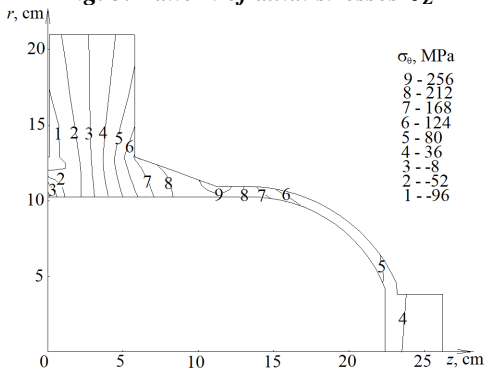

Fig. 4. Pattern of circumferential stresses σ_θ

SIFs are calculated by the interpolation method [11, 12] to determine local characteristics in the crack tip by the pattern of stresses in the body without a crack.

The crack growth rate under cyclic loading is computed in the *m*-th tip of the crack by Paris' formula

$$V_N^m = \frac{dl}{dN} = C_N \left(\Delta K_{\mathrm{I}}^m\right)^{n_N}, \qquad (2)$$

where ΔK_{I}^m is the maximum SIF range in the cycle; C_N, n_N are physical constants of the material, which are found experimentally:

$$\Delta K_{\mathrm{I}}^m = K_{\mathrm{Imax}}^m - K_{\mathrm{Imin}}^m ,$$

where K_{Imax}^m, K_{Imin}^m are the maximum and minimal SIF values of the normal opening mode in the cycle computed for the *m*-th tip of the crack.

Crack kinetics is computed by the Euler integration step method with automatic step selection.

Structure durability time is defined as the minimal time for the SIF range to reach its critical fracture toughness value under cyclic loading corresponding to the onset of avalanche-like fracture of the structure. Here, the crack dimensions are taken to be critical l_{cr} and (or) c_{cr}.

Research has experimentally proven that the structure strength depends on the environment [13, 14]. Changing ambient conditions has the utmost effect on local fracture processes both in the crack tip and on the rate of subcritical crack growth.

The kinetics of the semi-elliptical crack emerging on the internal surface of the electrolyser chamber wall was studied under static and cyclic loading. The initial crack dimensions (ellipse semi-axes) were l=0.5 mm and c=1 mm.

Fig. 6 shows the accepted crack growth rate dependence from SIF under static loading of steel. The dark spots show the dependence for gaseous hydrogen with 90 % humidity, and the light ones are for gaseous hydrogen with 15% humidity. The solid curve shows the dependence under electric hydrogenation conditions with a current density of 1.0 A/dm^2, and the dashed line is for a current density of 0.1 A/dm^2. Fig. 6 suggests that the current density, when it decreases by 10 times, reduces the crack growth rate by maximum 20%. In our case, the current density is approximately 1.0 A/dm^2. A crucial factor is that, at K_{I}>21 MPa$\sqrt{\mathrm{m}}$, the crack growth rate is virtually independent of the load magnitude. At K_{I}< 21 MPa$\sqrt{\mathrm{m}}$, the crack growth rate changes rapidly by more than 100 times, and at the threshold value of $K_{\mathrm{I}} \approx$ 15 MPa$\sqrt{\mathrm{m}}$ the crack stops growing under static loading.

Under cyclic loading, the kinetic fatigue fracture diagram shown in Fig. 7 was accepted, and the respective material fracture toughness constants were C_N=5.07×10^{-11} and n_N=2.36 at a current density of 1.0 A/dm^2.

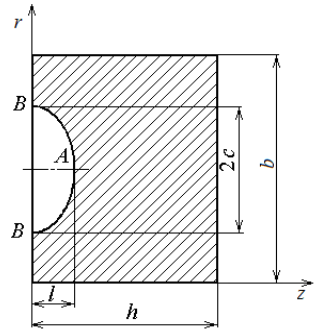

Fig. 5. Body cross-section in the plane of the semi-elliptical surface crack

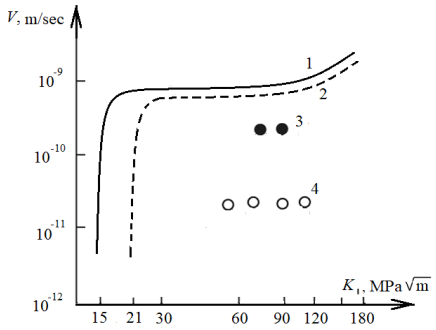

Fig. 6. Crack growth rate dependence from SIF under static loading of steel:
1 – with electrolytic hydrogenation at the current density 1.0 A/dm^2; 2 – with electrolytic hydrogenation at the current density 0.1 A/dm^2;
3 – in gaseous hydrogen with 90% humidity;
4 – in gaseous hydrogen with 15% humidity, T=20 ºC

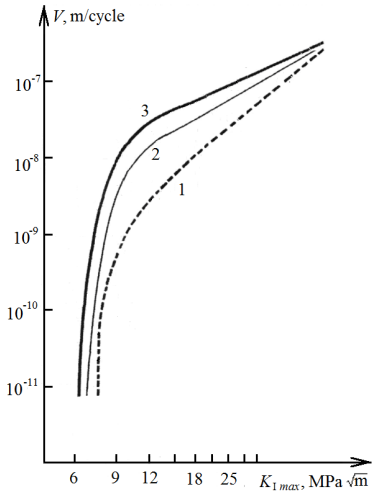

Fig. 7. Kinetic diagrams of fatigue fracture of steel:
1 – in air; 2, 3 – during electrolytic hydrogenation, current density, respectively, 0.1 and 1.0 A/dm^2

With the zero-to-tension cycle, the SIF threshold values were lower and about 6 MPa $\sqrt{\text{m}}$. At $K_{\text{I}} > 10$ MPa $\sqrt{\text{m}}$, the fatigue crack growth rate under cyclic loading is described with adequate accuracy by the Paris–Erdogan equation (2).

The kinetics of the surface meridional crack at the zero-to-tension loading cycle are shown in Figs. 8–9 and in table.

Therefore, if the structure has an initial defect (in our case, a meridional crack about 0.75 mm deep), it may grow at a rate of 0.06 mm/year.

At a meridional crack depth of about 0.3 mm and the given zero-to-tension cyclic loading, the crack will stop growing. When the crack depth is 1.75 mm, the crack will start growing not only due to cyclic loading with $N \approx 210$ cycles/year, but also owing to static loading under electrolytic hydrogenation conditions. Note that, with cyclic loading in air, the crack growth rate is roughly an order of magnitude smaller. With increasing crack depth, the rate will grow according to the graph in Fig. 8.

When the meridional crack depth is approximately 3 mm under static loading, the crack will start growing with a constant rate of 32 mm/year. In this case, even without cyclic loading, the crack will grow all the way through in about a month.

Conclusions

The developed method of simulating the stress-strain state based on the FEM was used for computational studies of the thermal stress state of the cover of an electrolyser cell. The method includes a software package for numerical analysis of the thermal stress state of structures with account of the complex geometry of objects, time-varying boundary conditions, heterogeneous properties of materials, and so forth. The validity of data returned by the developed computational method was confirmed by several test examples, as well as by the solution of a broad class of application problems [8].

The cylindrical part of the cover was found to be the most loaded one. The evaluation of the kinetics of the hypothetical crack in this domain demonstrates that, with a small number of cycles (less than 300 a year), the crack will grow for a long time (38 years) to a depth of 1.75 mm. After this, the rate of crack growth under static loading increases so rapidly that crack growth under cyclic loading may be neglected.

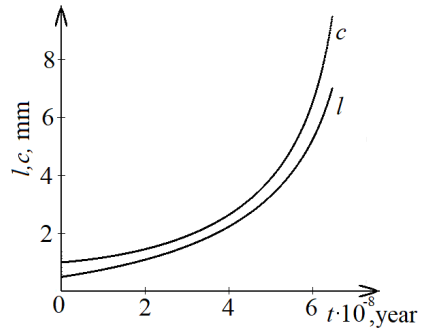

Fig. 8. Crack depth l and width c dependence from time

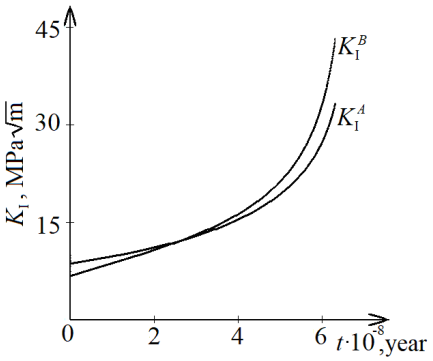

Fig. 9. SIF dependence in crack tips A and B from time

Dependence of SIF values in elliptical crack tips A and B from crack size

l, мм	c, мм	K_{I}^A, МПа $\sqrt{\text{м}}$	K_{I}^B, МПа $\sqrt{\text{м}}$
0.5	1	8.67	6.78
1.0	2	12.30	9.76
1.5	3	15.3	12.3
2.0	4	17.9	14.6
2.5	5	20.4	16.9
3.0	6	22.8	19.4
3.5	7	25.2	22.0
4.0	8	27.6	24.8
4.5	9	30.0	27.8
5.0	10	32.6	31.2

References

1. Solovei, V. V., Kotenko, A. L., Vorobiova, I. O., Shevchenko A. A., & Zipunnikov, M. M. (2018). Basic operation principles and control algorithm for a high-pressure membrane-less electrolyser. *Journal of Mechanical Engineering*, vol. 21, no. 4, pp. 57–63. https://doi.org/10.15407/pmach2018.04.057.
2. Tarzimoghadam, Z., Ponge, D., Klower, J., & Raabe, D. (2017). Hydrogen-assisted failure in Ni-based super alloy 718 studied under in situ hydrogen charging: The role of localized deformation in crack propagation. *Acta Materialia*, vol. 128, pp. 365–374. https://doi.org/10.1016/j.actamat.2017.02.059.
3. Ivaskevich, L. M., Balitskii, A. I., & Mochulskyi, V. M. (2012). Influence of hydrogen on the static crack resistance of refractory steels. *Materials Science*, vol. 48, no. 3, pp. 345–354. https://doi.org/10.1007/s11003-012-9512-z.

4. Balytskyi, O. I., Semerak, M. M., Balytska, V. O., Subota, A. V., Eliash, Ya., & Vus, O.B. (2013). *Zmina mitsnisnykh vlastyvostei vodnevykh baloniv na enerhoblokakh elektrostantsii za tryvaloi ekspluatatsii* [Strength properties change of hydrogen cylinders at power generating units of power plant for continuous operation]. *Pozhezhna bezpeka – Fire safety*, vol. 23, pp. 20–28 (in Ukrainian).
5. Balitskii, A. I. & Ivaskevich, L. M. (2018). Assessment of hydrogen embitterment in high-alloy chromium-nickel steels and alloys in hydrogen at high pressures and temperatures. *Strength of Materials*, vol. 50, pp 880–887. https://doi.org/10.1007/s11223-019-00035-2.
6. Dmytrakh, I. M., Leshchak, R. L., Syrotyuk, A. M., & Barna, R. A. (2017). Effect of hydrogen concentration on fatigue crack growth behavior in pipeline steel. *International Journal of Hydrogen Energy*, vol. 42, iss. 9, pp. 6401–6408. https://doi.org/10.1016/j.ijhydene.2016.11.193.
7. Ovchinnikov, I. I. & Ovchinnikov, I. G. (2012). *Vliyaniye vodorodosoderzhashchey sredy pri vysokikh temperaturakh i davleniyakh na povedeniye metallov i konstruktsiy iz nikh* [Effect of hydrogen-containing environment at high temperature and pressure on the behavior of metals and structures]. *Naukovedeniye – Eurasian Scientific Journal*, no. 4, pp. 1–28 (in Russian).
8. Shulzhenko, N. G., Gontarovskiy, P. P., & Zaytsev, B. F. (2011). *Zadachi termoprochnosti, vibrodiagnostiki i resursa energoagregatov (modeli, metody, rezultaty issledovaniy)* [Problems of thermal strength, vibrodiagnostics and resource of power units (models, methods, results of research)]. Saarbrücken, Germany: LAP LAMBERT Academic Publishing GmbH & Co. KG, 370 p. (in Russian).
9. Shul'zhenko, M. G., Gontarovskyi, P. P., Garmash, N. G., & Melezhyk, I. I. (2010). Thermostressed state and crack growth resistance or rotors of the NPP turbine K-1000-60/1500. *Strength of Materials*, vol. 42, pp. 114–119. https://doi.org/10.1007/s11223-010-9197-1.
10. Shulzhenko, M. H., Hontarovskyi, P. P., Matiukhin, Yu. I., Melezhyk, I. I., & Pozhydaiev, O. V. (2011). *Vyznachennia rozrakhunkovoho resursu ta otsinka zhyvuchosti rotoriv i korpusnykh detalei turbin.* [Determination of estimated resource and evaluation of rotor life and body parts of turbines: Methodological guidelines. Regulatory document SOU-N MEV 0.1–21677681–52:2011: approved by the Ministry of Energy and Coal Mining of Ukraine: Effective as of 07.07.11. Kyiv: Ministry of Energy and Coal Mining of Ukraine (in Ukrainian).
11. Ovchinnikov, A. V. (1988). An interpolation method of calculation of stress intensity factors. *Strength of Materials*, vol. 20, pp. 710–717. https://doi.org/10.1007/BF01530081.
12. (1995). *Pravila sostavleniya raschotnykh skhem i opredeleniye parametrov nagruzhennosti elementov konstruktsiy s vyyavlennymi defektami* [Rules for drawing up design schemes and determining the parameters of loading of structural elements with identified defects]: The Guidelines No. MR 125-02-95. Moscow: CNIITMASH, 52 p. (in Russian).
13. Cherepanov, G. P. (1979). Mechanics of Brittle Fracture. New York; London: McGraw-Hill.
14. Balytskyi, O. I., Makhnenko, O. V., Balytskyi, O. O., Hrabovskyi, V. A., Zaverbnyi, D. M., & Timofieiev B. T. (2005). *Mekhanika ruinuvannia i mitsnist materialiv* [Mechanics of fracture and strength of materials]: The reference guide. *T. 8. Mitsnist materialiv i dovhovichnist elementiv konstruktsii atomnykh elektrostantsii* [Vol. 8. Strength of materials and durability of structural elements of nuclear power plants]. Kyiv: Akademperiodyka Publishing House, 534 p. (in Ukrainian).

Received 28 August 2020

Аналіз росту тріщини в стінці електролізерної камери

П. П. Гонтаровський, Н. В. Сметанкіна, Н. Г. Гармаш, І. І. Мележик

Інститут проблем машинобудування ім. А. М. Підгорного НАН України,
61046, Україна, м. Харків, вул. Пожарського, 2/10

Електролізерні установки широко застосовуються у різних галузях промисловості. Вони представляють собою ємності високого тиску з камерою та розміщеними у ній електродами, які скомпоновані в пакети, а також кришку і патрубки. До їхніх технічних характеристик пред'являються високі вимоги, що підтверджують актуальність проблеми удосконалення методів досліджень. Для моделювання кінетики термонапруженого стану в елементах енергоустановок зі складними реологічними характеристиками матеріалу й з урахуванням його пошкоджуваності на базі методу скінченних елементів розроблена спеціальна методика й програмний комплекс, що дозволяють у тривимірній постановці розв'язувати широкий клас нелінійних нестаціонарних задач із одночасним урахуванням усіх чинних факторів. Дослідження кінетики тріщини виконані з використанням методики розрахункової оцінки живучості елементів конструкцій, яка базується на принципах механіки крихкого руйнування,

при цьому зона пластичності у вершині тріщини приймається малою у порівнянні з розмірами тріщини, а кінетика тріщини визначається коефіцієнтами інтенсивності напружень у її вершинах. Методика ґрунтується на розрахунках кінетики тріщини до критичних розмірів, коли відбувається лавиноподібне руйнування елемента конструкції, або тріщина проростає наскрізь по товщині елемента. Кінетика напівеліптичної тріщини, яка виходить на внутрішню поверхню стінки електролізерної камери, досліджувалася під дією статичного й циклічного навантажень. Із використанням розробленої методики виконані розрахункові дослідження термонапруженого стану верхньої частини електролізерної комірки. Отримані результати показують, що циліндрична частина кришки є найбільш навантаженою. Виконані дослідження розвитку внутрішньої поверхневої напівеліптичної тріщини, яка зародилася в цій зоні. Установлено, що при малій кількості циклів за рік тріщина буде довго підростати до певної глибини, далі швидкість її росту від статичного навантаження збільшується так швидко, що ростом тріщини від циклічного навантаження можна знехтувати.

***Ключові слова**: електролізер, наводнювання, напружено-деформований стан, середа, тріщина.*

Література

1. Solovei V. V., Kotenko A. L., Vorobiova I. O., Shevchenko A. A., Zipunnikov M. M. Basic operation principles and control algorithm for a high-pressure membrane-less electrolyser. *J. Mech. Eng*. 2018. Vol. 21. No. 4. P. 57–63. https://doi.org/10.15407/pmach2018.04.057.
2. Tarzimoghadam Z., Ponge D., Klower J., Raabe D. Hydrogen-assisted failure in Ni-based superalloy 718 studied under in situ hydrogen charging: the role of localized deformation in crack propagation. *Acta Materialia*. 2017. Vol. 128. P. 365–374. https://doi.org/10.1016/j.actamat.2017.02.059.
3. Ivaskevich L. M., Balitskii A. I., Mochulskyi V. M. Influence of hydrogen on the static crack resistance of refractory steels. *Materials Sci*. 2012. Vol. 48. No. 3. P. 345–354. https://doi.org/10.1007/s11003-012-9512-z.
4. Балицький О. І., Семерак М. М., Балицька В. О., Субота А. В., Еліаш Я., Вус О.Б. Зміна міцнісних властивостей водневих балонів на енергоблоках електростанцій за тривалої експлуатації. Пожежна безпека. 2013. Т. 23. С. 20–28.
5. Balitskii A. I., Ivaskevich L. M. Assessment of hydrogen embrittlement in high-alloy chromium-nickel steels and alloys in hydrogen at high pressures and temperatures. *Strength Materials*. 2018. Vol. 50. P. 880–887. https://doi.org/10.1007/s11223-019-00035-2.
6. Dmytrakh I. M., Leshchak R. L., Syrotyuk A. M., Barna R. A. Effect of hydrogen concentration on fatigue crack growth behavior in pipeline steel. *Intern. J. Hydrogen Energy*. 2017. Vol. 42. Iss. 9. P. 6401–6408. https://doi.org/10.1016/j.ijhydene.2016.11.193.
7. Овчинников И. И., Овчинников И. Г. Влияние водородосодержащей среды при высоких температурах и давлениях на поведение металлов и конструкций из них. *Науковедение.* 2012. № 4. С. 1–28.
8. Шульженко Н. Г., Гонтаровский П. П., Зайцев Б. Ф. Задачи термопрочности, вибродиагностики и ресурса энергоагрегатов (модели, методы, результаты исследований). Saarbrucken, Germany: LAP LAMBERT Academic Publishing GmbH & Co. KG, 2011. 370 с.
9. Shul'zhenko M. G., Gontarovskyi P. P., Garmash N. G., Melezhyk I. I. Thermostressed state and crack growth resistance or rotors of the NPP turbine K-1000-60/1500. *Strength Materials*. 2010. Vol. 42. P. 114–119. https://doi.org/10.1007/s11223-010-9197-1.
10. Визначення розрахункового ресурсу та оцінка живучості роторів і корпусних деталей турбін. Методичні вказівки: СОУ- Н МЕВ 40.1–21677681– 52:2011 / М. Г. Шульженко, П. П. Гонтаровський, Ю. І. Матюхін, І. І. Мележик, О. В. Пожидаєв. К.: ОЕП «ГРІФРЕ»: М-во енергетики та вугільної промсті України, 2011. 42 с.
11. Ovchinnikov A. V. An interpolation method of calculation of stress intensity factors. *Strength Materials*. 1988. Vol. 20. P. 710–717. https://doi.org/10.1007/BF01530081.
12. Методические рекомендации МР 125-02-95. Правила составления расчётных схем и определение параметров нагруженности элементов конструкций с выявленными дефектами. М.: ЦНИИТМАШ, 1995. 52 с.
13. Черепанов Г. П. Механика хрупкого разрушения. М.: Наука, 1974. 640 с.
14. Механіка руйнування і міцність матеріалів: Довід. посіб. / Під заг. ред. В. В. Панасюка. Т. 8: Міцність матеріалів і довговічність елементів конструкцій атомних електростанцій / О. І. Балицький, О. В. Махненко, О. О. Балицький, В. А. Грабовський, Д. М. Завербний, Б. Т. Тімофєєв. Під ред. О. І. Балицького. Київ: ВД «Академперіодика», 2005. 534 с.